Published in final edited form as:
Ultrasound Med Biol. 2008 January ; 34(1): 31–39.

In vivo cardiac imaging of adult zebrafish using high frequency ultrasound (45–75 MHz)

Lei Sun[1,*], **Ching-Ling Lien**[2], and **K. Kirk Shung**[1]

1 *Department of Biomedical Engineering, University of Southern California, 1042 Downey Way, DRB 132, Los Angeles, CA 90089*

2 *Department of Cardiothoracic Surgery, Childrens Hospital Los Ageles and University of Southern California, 4650 Sunset Blvd. MS#137, Los Angeles, CA 90027*

Abstract

The zebrafish has emerged as an excellent genetic model organism for studies of cardiovascular development. Optical transparency and external development during embryogenesis allow for visual analysis in the early development. However, to understand the cardiovascular structures and functions beyond the early stage requires a high-resolution, real-time, non-invasive imaging alternative due to the opacity of adult zebrafish. In this research, we report the development of a high frequency ultrasonic system for adult zebrafish cardiac imaging, capable of 75 MHz B-mode imaging at a spatial resolution of 25 μm and 45 MHz pulsed-wave Doppler measurement. The system allows for real-time delineation of detailed cardiac structures, estimation of cardiac dimensions, as well as image-guided Doppler blood flow measurements. *In vivo* imaging studies showed the identification of the atrium, ventricle, bulbus arteriosus, atrioventricular valve, and bulboventricular valve in real-time images, with cardiac measurement at various stages. Doppler waveforms acquired at the ventricle and the bulbus arteriosus demonstrated the utility of this system to study the zebrafish cardiovascular hemodynamics. This high frequency ultrasonic system offers a multitude of opportunities for cardiovascular researchers. In addition, the detection of E-flow and A-flow during the ventricular filling, and the appearance of diastolic flow reversal at bulbus arteriosus suggested the functional similarity of zebrafish heart to that of higher vertebrates.

Keywords

high frequency ultrasound; ultrasound bio-microscopy; pulsed-wave Doppler; zebrafish; echocardiography

INTRODUCTION

The zebrafish has emerged as an excellent genetic model organism for studies of cardiovascular development (Chen et al. 1996; Serbedzija et al. 1998; Thisse and Zon 2002), primarily due to its small size, fecundity, and brief generation time (Patton and Zon 2001). Additionally, the zebrafish heart shares a common structural scenario with a mammalian heart, and, as such, can serve as a model for various experimental studies (Weinstein and Fishman 1996). Furthermore,

Please send correspondence to: Lei Sun, Ph.D., Department of Biomedical Engineering, Viterbi School of Engineering, University of Southern California, 1042 Downey Way, Denney Research Building (DRB) 132, Los Angeles, CA 90089, Fax: (213) 821-3897, Phone: (213) 821-2651, Email: sunlei@usc.edu.

optical transparency and external development during embryogenesis allow for visual analysis of the early developmental process. However, optical methods are not suitable for the study of adult zebrafish due to the opacity beyond its early stage. Histology (Hu et al. 2000; Hu et al. 2001), scanning electron microscopy (SEM) and transmission electron microscopy (Hu et al. 2001) were applied to evaluate the cardiac morphology in fixed adult zebrafish hearts, without providing *in vivo* data. Magnetic resonance microscopy (Kabli et al. 2006) was used to examine anatomical structures in adult zebrafish *ex vivo* and *in vivo*, but the image acquisition took a long period of time (128 to 480 seconds). A conventional ultrasonic imaging device was employed to image the heart of adult zebrafish at 7 and 8.5 MHz (Ho et al. 2002), but the resolution was inadequate and useful observations of zebrafish cardiac functions were difficult. High frequency ultrasonic imaging on adult zebrafish has also been studied (Sun et al. 2006), but the linear mechanical scan up to 5 frames per second (fps) restricted the imaging speed and limited the capability of real-time visualization of the beating heart. Currently, there is a lack of a high resolution, real-time, non-invasive imaging tool for the assessment of zebrafish cardiovascular morphology and functions.

Ultrasound bio-microscopy (UBM) is based on the same fundamental principles as conventional clinical ultrasonic scanners but produces images with higher spatial resolution because of the utilization of higher center frequencies. Current UBM systems can also provide blood flow estimation at a sensitivity of a few millimeters per second in the microcirculation (Foster et al. 2002). Using a 40-MHz UBM system, *in vivo* investigation on mouse embryos has been carried out to detect detailed cardiac structures and slow blood flows (Aristizabal et al. 1998; Foster et al. 2002; Srinivasan et al. 1998). For *in vivo* cardiac imaging in zebrafish, whose heart is approximately 1 mm in diameter, a real-time UBM with higher center frequencies could be an option and may offer adequate resolutions to facilitate the study of the cardiovascular functions and physiology.

In this paper, we report the development and the utility of a duplex UBM system for adult zebrafish cardiovascular investigation, with the capabilities of 75 MHz B-mode imaging and 45 MHz pulsed-wave Doppler measurement. The construction of the system is first described, followed by a discussion on wire phantom testing showing that the axial and lateral resolutions of this system are 25 μm and 56 μm, respectively. *In vivo* studies in 10 adult zebrafish were carried out using this duplex UBM system. Representative images and Doppler waveforms from various cardiac structures are given to demonstrate the applications of this system for cardiovascular research in zebrafish.

MATERIALS AND METHODS

UBM Imaging Instruments

The block diagram of the duplex UBM system for zebrafish imaging is shown in Figure 1. The system consisted of a novel high speed mechanical sector probe and a digitally implemented servo controller (Capistrano Labs Inc, San Clemente, CA). It was capable of producing up to 200 frames of B-mode images per second; details were described previously (Sun et al. 2007). A photo of the sector probe and servo control board is shown in Figure 2. A position-based triggering scheme was implemented in a complex programmable logic device (CPLD) chip to ensure that an image was composed of equally spaced scan lines (37 μm spacing at the focus is typical). The imaging front-end electronics consisted of a customized high frequency bipolar pulse generator (Xu et al. 2007), low noise amplifiers (AU-1114 and AU-1466, Miteq Inc, Hauppauge, NY), a band pass filter (BIF-70, Mini-Circuits, Brooklyn, NY), and an expander and limiter (Matec Instruments Company, Northborough, MA). The radio frequency (RF) echo signals were digitized by a 12-bit analog to digital converter with a sampling frequency of 400 MHz (CS12400, Gage Applied Technologies, Inc., Lachine, QC, Canada). The digitized RF data were processed by envelop detection and log-compression algorithms,

followed by linear mapping to gray scale levels for display at a 60 dB dynamic range. All images and digitized RF data were stored in a hard drive of a computer for later reference.

A 75 MHz light-weight (0.2 g) spherically focused transducer was fabricated for this study using lithium niobate. It had an aperture of 2 mm, with a focal distance of 5 mm (Fig. 3a). The finished transducers produced a pulse-echo response centered at 75 MHz with a −6dB bandwidth of 60% (Fig. 3b). The theoretical axial resolution R_{ax} and lateral resolution R_{lat} of a focused ultrasound transducer can be expressed by the following equations (Foster et al. 2000):

$$R_{ax} = \frac{1}{2} * \frac{c}{BW} \tag{1}$$

$$R_{lat} = \lambda * \frac{FD}{A} = \lambda * (f\_number) \tag{2}$$

where c is the speed of sound (1460 m/s in water), and BW is the bandwidth of the transducer (45MHz, 60% fractional BW), λ is the wavelength at the center frequency (19.5 μm at 75MHz), FD is the focal distance (5 mm), A is the diameter of the transducer (2 mm), f_number is defined as the ratio of the focal distance to the aperture dimension (2.5). According to equations (1) and (2), the theoretical axial and lateral resolutions were 16 μm and 48.5 μm, respectively.

The experimental spatial resolutions were obtained from a cross-sectional scan of an 8 μm (diameter) tungsten wire placed at the focus of the transducer (Fig. 4). This figure plots the spatial distribution of the relative pressure amplitude. The experimental axial and lateral resolutions are typically measured as the dimensions of −6 dB pressure distribution with respect to the peak amplitude. They were found to be 25 μm and 56 μm, respectively. The experimental spatial resolutions were in good agreement with the theoretical values discussed earlier. Finally, the compensated insertion loss was 18.5 dB. More information can be found elsewhere (Cannata et al. 2003;Sun et al. 2007).

Pulsed-wave Doppler System and Signal Processing

In addition to B-mode imaging, the system also incorporated a 45 MHz pulsed-wave Doppler. The schematics of the Doppler design are shown in Figure 5. It included a programmable clock generator (ECS-P83/P85, ECS Inc International, Kansas City, KS) as a master oscillator producing a 45MHz reference signal. A gate control component determined the sample depth and sample volume. A demodulator (MIQC-60WD, Mini-Circuits, Brooklyn, NY) acquired the in-phase (I_{IF}) and quadrature-phase (Q_{IF}) signals. After digitization and processing of the I_{IF} and Q_{IF} signals, the Doppler waveforms were obtained and displayed, with the Doppler sound played by a stereo speaker simultaneously. Finally, the Doppler waveforms were stored in a computer for later reference. The Doppler waveforms were estimated using the method described by Jensen (1996):

$$v = \frac{\Delta f}{2 f_0 \cos\theta} c \tag{3}$$

where Δf is the measured Doppler shift frequency, f_0 is the center frequency of the transducer (45 MHz), c is the sound velocity in soft tissue (1540 m/s), and θ is the angle between the ultrasound beam and the flow, estimated from B-mode images.

For proper temporal and velocity resolutions, the number of points for spectral analysis should be selected carefully to ensure the Doppler waveforms had adequate velocity and temporal

resolutions. According to Jensen (1996), the minimal detectable velocity (velocity resolution) can be expressed as the following equation:

$$v_{\min} = \frac{c}{2} * \frac{f_{prf}}{N f_0} \tag{4}$$

where c is the speed of sound (1540 m/s), f_{prf} is the pulse repetition frequency (11KHz), f_0 is the center frequency of the transmitted Doppler pulses (45MHz), N is the number for points. The temporal resolution can be expressed as:

$$T_{\min} = \frac{N}{f_{prf}} * (1 - OL) \tag{5}$$

where OL is the temporal overlap in percentage (%) between two consecutive windows of spectral analysis. The display update rate will be $1/T_{min}$. Suggested by Christopher et al. (1997), number of points N should be selected so that the Doppler waveform within each cardiac cycle contained at least 25 lines of data points, and the peak-to-peak velocity range should contain similar number of lines of data points. Values of N, velocity resolution, and temporal resolution for the following Doppler measurement are given in the Results section.

Animal

The animal experiments were performed with a protocol approved by the Institutional Animal Care and Use Committee (IACUC) at the University of Southern California. Zebrafish were obtained from Aquatica Tropicals (Aquatica Tropicals, Plant City, FL) and maintained in a recirculating aquarium system at temperature of 25°C. The fish were fed twice daily with flake food (OmegaSea Ltd., Perry, OH). A total of ten one-year-old wild type zebrafish were studied, with a body length from 3 to 4 cm. During *in vivo* experiments, the fish were anesthetized by placed at 0.08% tricaine solution (MS-222, Ethyl 3-aminobenzoate methanesulfonate salt (Sigma-Aldrich, St. Loius, MO)) for 30 seconds, followed by gently removing the scales at the ventral side between the gills. Afterwards, the fish were maintained in 0.04% tricaine solution throughout the experiments. All the studies were performed at temperature of 27.5°C for less than 20 minutes. Following the procedures the animals were euthanized by placing them in 1% tricaine solution for 15 minutes.

In vivo UBM Imaging and Doppler Measurement

Each zebrafish was placed upside down in a small rubber holder submerged in a plastic container filled with the tricaine solution. The container was put on a two-axis manual positioner (Optosigma Corporation, Santa Ana, CA) for a precise imaging plane alignment. The ultrasound probe was attached to a holder and lowered into the solution with 3 mm clearing distance to the fish skin. The probe was rotated and fixed at different positions to acquire images along various planes. The transducer was scanned over a sector-shaped area of 4 mm by 4 mm at a frame rate up to 200 images per second. The high frame capability facilitated the visualization of heart wall and valve motion, and improved the accuracy of measurements of heart chamber dimensions and their variations over the heart cycle. Real-time images were displayed, with the desired ones captured and saved in a personal computer.

During the acquisition of Doppler waveforms, the transducer was stopped at a fixed angle. The sample depth was predetermined as the focal distance of the transducer (5 mm), with a length of sample volume as 115 μm. The length of the sample volume is adjustable by jumpers in the hardware setting. Considering the size of a zebrafish heart to be 1 to 2 mm, the selection of 115 μm sample volume length allowed adequate spatial resolution and good detectability of small vessels. The pulse repetition frequency (PRF) was chosen to be 11 KHz. Under the

guidance of real-time images, the Doppler signals were acquired with an estimation of the Doppler angle. Doppler waveforms from ventricle and bulbus arteriosus were captured, and digitized by an audio card and saved in a personal computer hard drive.

RESULTS AND DISCUSSION

Zebrafish heart consisted of an atrium and a ventricle, which are connected to the sinus venosus and bulbus arteriosus (Hu et al. 2001). Despite its apparent simplicity, the zebrafish heart shares a common structural scenario with a human heart. Figures 6a–6b shows sagittal and transverse views of the atrium and ventricle, respectively. The heart was located medially on the ventral side between the gills right under the skin. The atrium is displayed underneath the ventricle slightly to the right on its dorsal side, simply because the fish was placed upside down. The cardiac dimensions at the isovolumic relaxation stage were 1.2 mm by 1.6 mm. From Figure 6b, it is noted that the dimensions of the atrium (0.81 × 0.58 mm) and ventricle (1.19 × 0.62 mm) were similar, which agreed with the observation by Hu et al. (2001). The SEM image in Hu et al. (2001) indicated similar dimensions between the atrium and the ventricle. This fact may indicate that the zebrafish atrium plays a different role than that in humans. Table 1 summarizes the zebrafish cardiac dimensions at isovolumic relaxation (IVR) and isovolumic contraction (IVC) stages. In addition, in real-time images (video clip 1 and 2), the cyclic contraction of the atrium followed by the ventricle was recognized as each chamber became a brighter structure in a sequential manner. In a slow-motion movie, the sequence of this diastole-systole contraction became more apparent (video clip 3 and 4).

Under the UBM guidance, the ventricular blood flow was measured, with the Doppler waveform shown in Figure 6c. It demonstrates a characteristic inflow-outflow pattern, with a sharp-peaked, high velocity inflow waveform followed by a broad-peaked, lower velocity outflow waveform. The inflow occurred during the ventricular filling as the blood flowed toward the transducer, corresponding to the positive Doppler waveform. It consisted of early diastolic filling (E) and late diastolic filling (A). During E-flow where ventricular pressure falls below atrial pressure due to ventricular relaxation, the atrioventricular (AV) valve, between the atrium and the ventricle, opens and the blood flows from atrium to ventricle. During atrial contraction, the atrial pressure exceeds the ventricular pressure, resulting in a second AV valve opening and late diastolic A-flow. Form Doppler measurement, the peak E and A velocities were 3.6 cm/s and 14.4 cm/s, respectively, at an estimated 60° Doppler angle. The number of data points for spectral analysis was 256. The velocity resolution was 0.7 mm/s and the temporal resolution was 11.6 ms. The E/A ratio, defined as the E velocity divided by A velocity, was 0.25, which agreed with the observations by Ho et al. (2002). However, the E/A ratio is significantly smaller than that in humans. This might again suggest that the zebrafish atrium plays a different role than that in higher vertebrates. The time duration of E-flow and A-flow were 320 ms and 110 ms, respectively. At ventricular systole, the bulboventricular (BV) valve opened and the blood flowed from the ventricle to the bulbus arteriosus. This was represented as the ventricular outflow, corresponding to the negative Doppler waveform. The peak velocity of the outflow was 8.0 cm/s with a duration of 200 ms. In addition, a cardiac cycle was found to be 650 ± 175 ms (mean ± SD), corresponding to a heart rate of 93 ± 25 beats per minute (mean ± SD).

Figure 7a shows a zebrafish heart in a sagittal view at the isovolumic contraction stage. Major cardiac structures were detected, including the ventricle, bulbus arteriosus (BA), atrioventricular (AV) valve, bulboventricular (BV) valve, and epicardium. The AV and BV valves were in closed position as two bright bands extended between cardiac chambers, which can be clearly seen in the real-time images (video 5). The AV valve is positioned medially on the dorsal side of the ventricle. The BV valve is located at the anterior portion of the ventricle connected to the bulbus arteriosus. It is noted that the dimension of the ventricle increased

significantly compared to that at end systole (Fig. 6a). A series of transverse views of the BV valve are shown in Figures 7b-d from open to closed positions, with a time interval of 60 ms. The BV valve appeared to be a long structure with one end fixed at the left epicardium and the other end moving ventrally. In real-time images (video clip 6), they could be easily recognized by their characteristic motion. The epicardium looked very bright, possibly because the ultrasonic beam was propagating perpendicular to that tissue.

Doppler waveforms at the medial and posterior bulbus arteriosus were acquired and displayed in Figures 7e and 7f. At the medial bulbus arteriosus, the blood flow pattern was unidirectional, with a peak velocity of 16.0 cm/s at 60° Doppler angle (Fig. 7e). While at the posterior bulbus arteriosus, close to the BV valve, not only did the peak velocity of systolic forward flow increase (18.0 cm/s), but the diastolic flow reversal (DFR) appeared (Fig. 7f). The DFR was caused during diastole when the ventricular pressure dropped below that of bulbus arteriosus and the blood flowed backward toward the ventricle. The number of data points for spectral analysis was 128. The velocity resolution was 1.38 mm/s and the temporal resolution was 5.8 ms. Finally, the peak velocities and time durations measured from Doppler waveform in 10 fishes are listed in Table 2 (mean ± SD).

B-mode imaging and Doppler measurement were conducted on the same transducer at 75MHz and 45MHz, respectively. The pulsed-wave Doppler electronics was designed and optimized at 45MHz. At this frequency, it had optimal performance with minimal noise level, good sensitivity and adjustability. In addition, the bandwidth of the transducer was broad enough that a reduced sensitivity of 10 dB at 45MHz did not significantly degrade the Doppler measurement. Doppler waveforms shown in Figures 6c, 7e and 7f displayed large SNR, good velocity and temporal resolutions, demonstrating good behavior of the Doppler system working off the center frequency.

CONCLUSION

A high frequency ultrasonic system for real-time, noninvasive cardiovascular assessment in adult zebrafish *in vivo* has been developed at a spatial resolution of 25 μm. This UBM system is capable of 75 MHz B-mode imaging and 45 MHz pulsed-wave Doppler measurement, which allows for real-time delineation of detailed cardiac structures, estimation of cardiac dimensions, as well as image-guided Doppler blood flow measurements. Major structures in the zebrafish heart were detected using this scanner, allowing dimensional analysis of the atrium and ventricle. Image-guided blood flow measurement from the ventricle and bulbus arteriosus were carried out, with an estimation of peak velocities, time durations and heart rates. The acquired Doppler waveforms displayed a high similarity to those measured in humans, and suggested the functional resemblance of zebrafish heart to that of higher vertebrates. The relatively large atrial dimensions and significantly small E/A ratio may indicate that the zebrafish atrium plays a different role in the cardiovascular system. These results demonstrate the utility of real-time, noninvasive cardiovascular evaluation of the adult zebrafish heart *in vivo* using high frequency ultrasound. This system may help longitudinal studies of disease prognosis, and become a useful tool to investigate mutant and transgenic zebrafish to understand the genotype-phenotype relationship.

Supplementary Material

Refer to Web version on PubMed Central for supplementary material.

Acknowledgements

The authors would like to thank the National Institutes of Health (NIH) for financial support through Grant 1R01HL079976, and Ruibin Liu for fabricating the 75 MHz light-weight transducer.

References

Aristizabal O, Christopher DA, Foster FS, Turnbull DH. 40-MHz echocardiography scanner for cardiovascular assessment of mouse embryos. Ultrasound Med Biol 1998;24:1407–1417. [PubMed: 10385963]

Cannata JM, Ritter TA, Chen W, Silverman RH, Shung KK. Design of efficient, broadband single-element (20–80 MHz) ultrasonic transducers for medical imaging applications. IEEE Trans Ultrason Ferroelect Freq Contr 2003;50:1548–1557.

Chen JN, Haffter P, Odenthal J, Vogelsang E, Brand M, van Eeden FJM, Furutani-Seiki M, Granato M, Heisenberg MC, Jiang YJ, Kane DA, Kelsh RN, Mullins MC, Nusselein-Volhard C. Mutation affecting the cardiovascular system and other internal organs in the zebrafish embryo. Development 1996;123:293–302. [PubMed: 9007249]

Christopher DA, Burns PN, Starkoski BG, Foster FS. A high-frequency pulsed-wave Doppler ultrasound system for the detection and imaging of blood flow in the microcirculation. Ultrasound Med Biol 1997;23:997–1015. [PubMed: 9330444]

Foster FS, Pavlin CJ, Harasiewicz KA, Christopher DA, Turnbull DH. Advances in ultrasound biomicroscopy. Ultrasound Med Biol 2000;26:1–27. [PubMed: 10687788]

Foster FS, Zhang MY, Zhou YQ, Liu G, Mehi J, Cherin E, Harasiewicz KA, Starkoski BG, Zan L, Knapik DA, Adamson SL. A new ultrasound instrument for in vivo microimaging of mice. Ultrasound Med Biol 2002;28:1165–1172. [PubMed: 12401387]

Ho YL, Shau YW, Tsai HJ, Lin LC, Huang PJ, Hsieh FJ. Assessment of zebrafish cardiac performance using Doppler echocardiography and power angiography. Ultrasound Med Biol 2002;28:1137–1143. [PubMed: 12401383]

Hu N, Sedmera D, Yost HJ, Clark EB. Structure and function of the developing zebrafish heart. Anat Rec 2000;260:148–157. [PubMed: 10993952]

Hu N, Yost HJ, Clark EB. Cardiac morphology and blood pressure in the adult zebrafish. Anat Rec 2001;264:1–12. [PubMed: 11505366]

Jensen, JA. Estimation of blood velocities using ultrasound. New York: Cambridge University Press; 1996.

Kabli S, Alia A, Spaink HP, Verbeek FJ, De Groot HJM. Magnetic resonance microscopy of the adult zebrafish. Zebrafish 2006;3:431–439. [PubMed: 18377223]

Patton EE, Zon LI. The art and design of genetic screens: zebrafish. Nat Rev Genet 2 2001;12:956–966.

Serbedzija GN, Chen JN, Fishman MC. Regulation in the heart field of zebrafish. Development 1998;125:1095–1101. [PubMed: 9463356]

Srinivasan S, Baldwin HS, Aristizabal O, Kwee L, Labow M, Artman M, Turnbull DH. Noninvasive, in utero imaging of mouse embryonic heart development with 40-MHz echocardiography. Circulation 1998;98:912–918. [PubMed: 9738647]

Sun L, Richard WD, Cannata JM, Ching F, Johnson JA, Yen JT, Shung KK. A high frame rate high frequency ultrasonic system for cardiac imaging in mice. IEEE Trans Ultrason Ferroelect Freq Contr. 2007to appear in August

Sun L, Sangkatumvong S, Shung KK. A high resolution digital ultrasound system for imaging of zebrafish. IEEE Ultrason Sympos 2006:2202–2205.

Thisse C, Zon LI. Organogenesis—Heart and blood formation from zebrafish point of view. Science 2002;295:457–462. [PubMed: 11799232]

Weinstein BM, Fishman MC. Cardiovascular morphogenesis in zebrafish. Cardiovasc Res 1996;31:17–24.

Xu X, Yen JT, Shung KK. A low-cost bipolar pulse generator for high-frequency ultrasound applications. IEEE Trans Ultrason Ferroelec Freq Contr 2007;54:443–447.

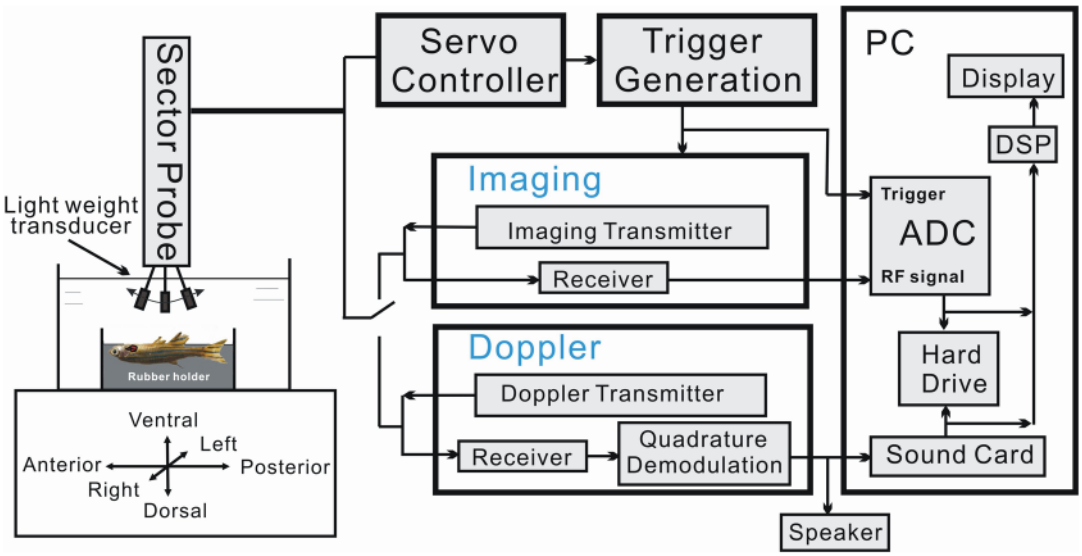

Figure 1.
Block diagram of a high resolution ultrasonic system for real-time, noninvasive cardiac imaging in adult zebrafish. This duplex system is capable of 75MHz B-mode imaging and 45 MHz pulsed-wave Doppler measurement.

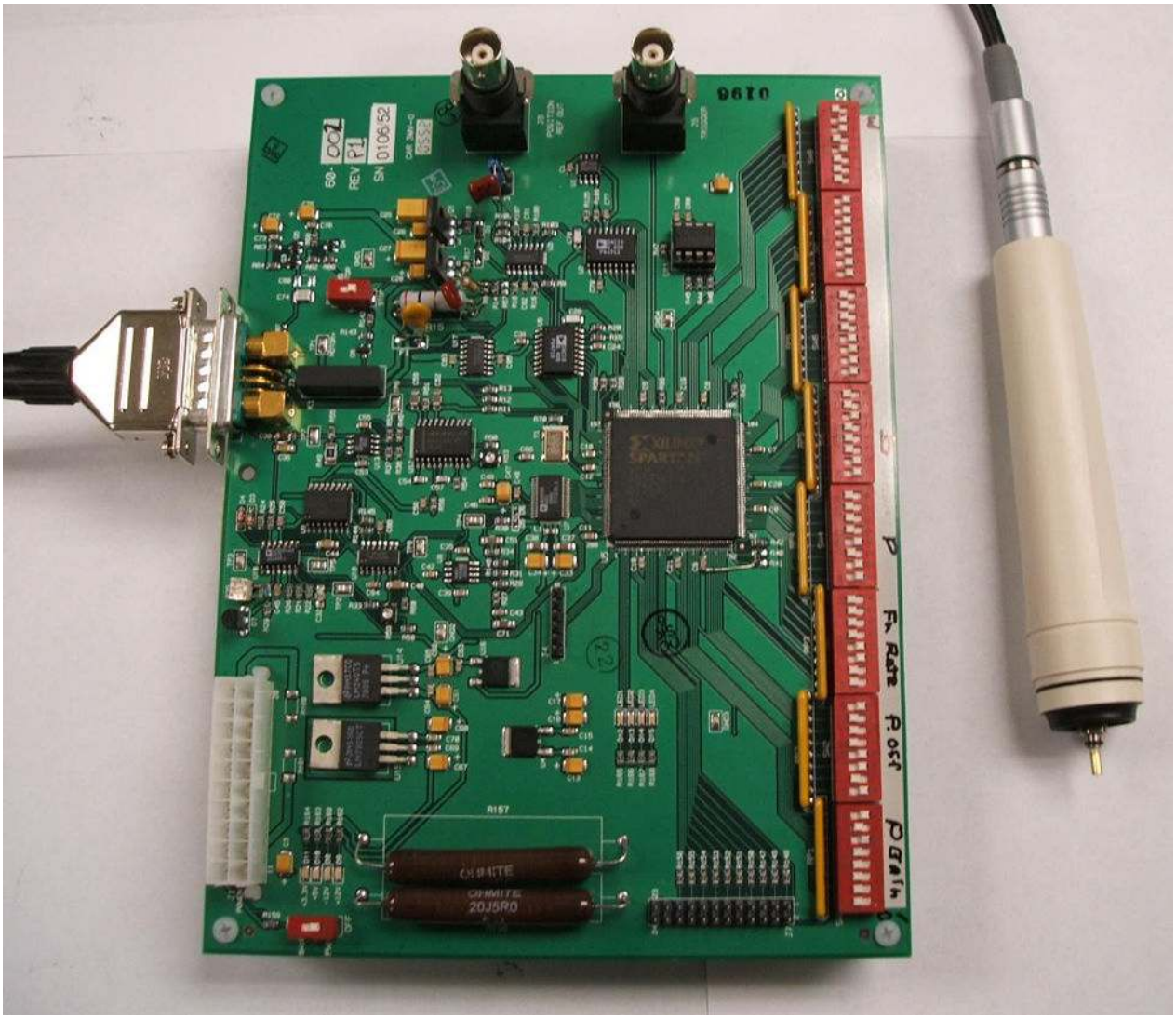

Figure 2.
A photo of the sector probe and digitally implemented servo control board.

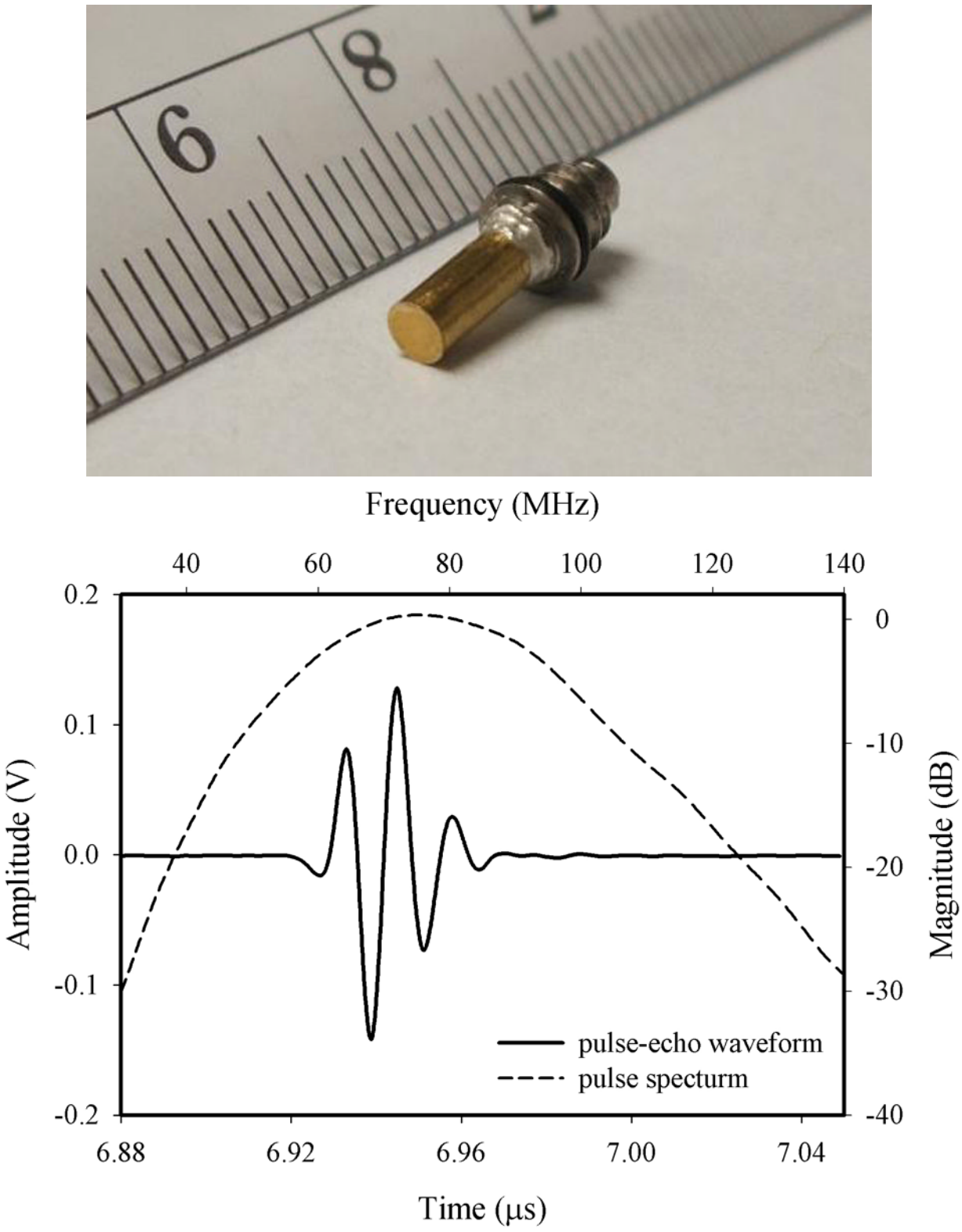

Figure 3.

(a) A photo of the 75MHz light-weight (0.2 g), spherically focused ultrasonic transducer used in this study. It had an aperture of 2 mm, focal distance of 5 mm, and a compensated insertion loss of 18.5 dB. (b) The normalized pulse-echo waveforms in time- and frequency- domain.

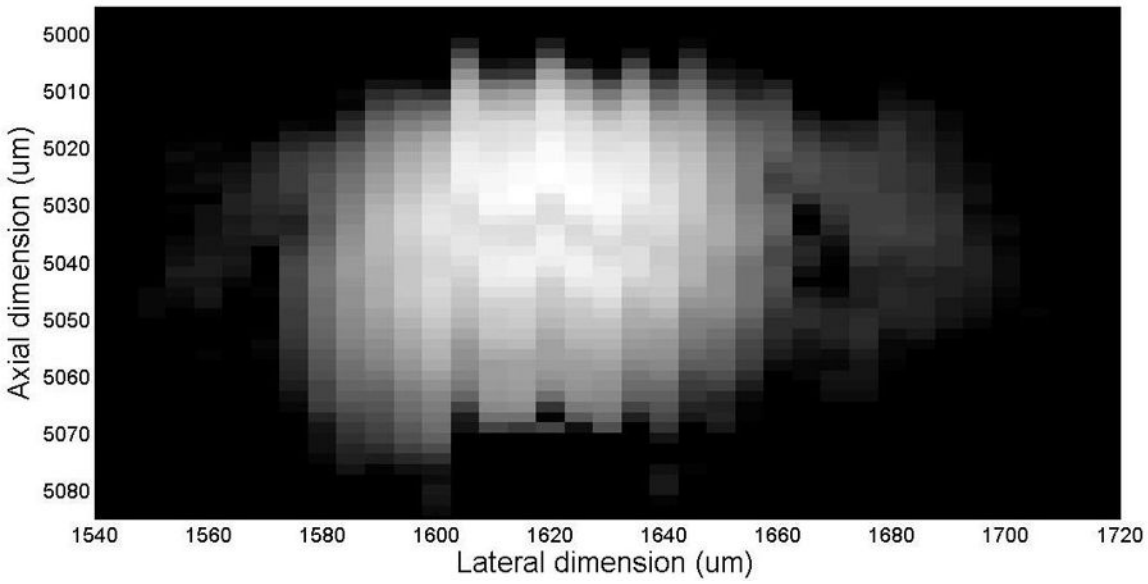

Figure 4.
Ultrasound image of a cross-sectional scan of an 8 μm tungsten wire at the transducer focus, displaying the spatial distribution of the relative pressure amplitude from the 75 MHz focused transducer.

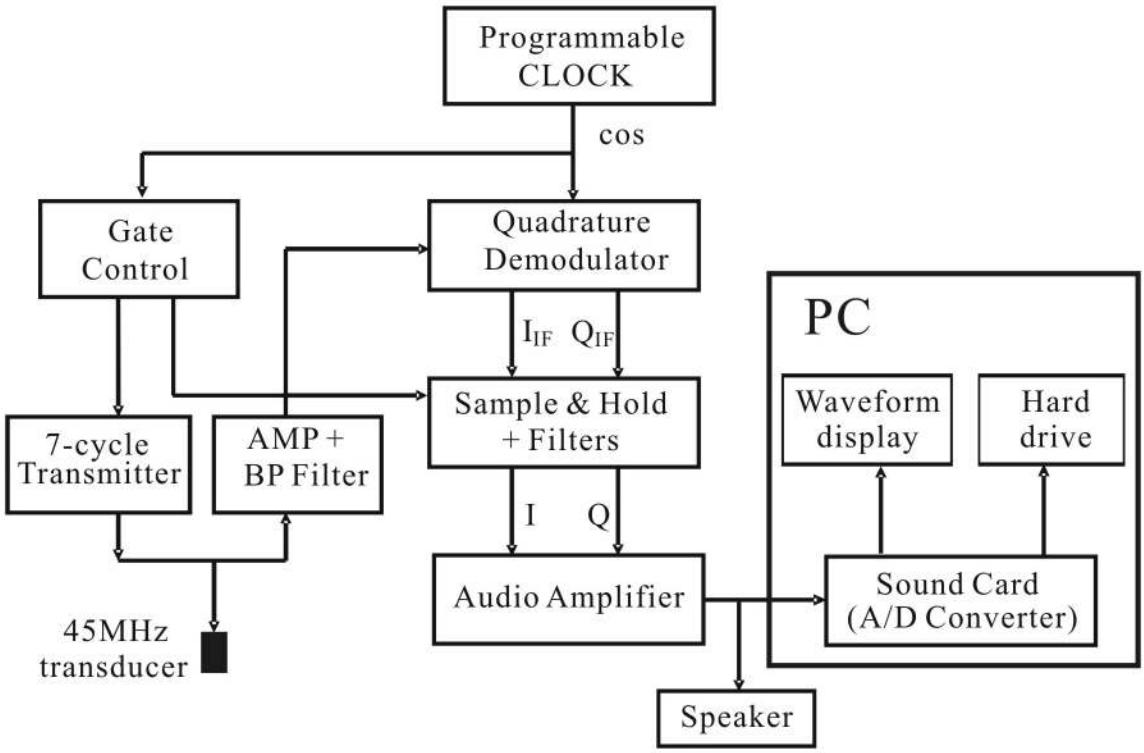

Figure 5.
Schematics of the 45MHz directional pulsed-wave Doppler system. The system was implemented in a low cost PCB-based circuit.

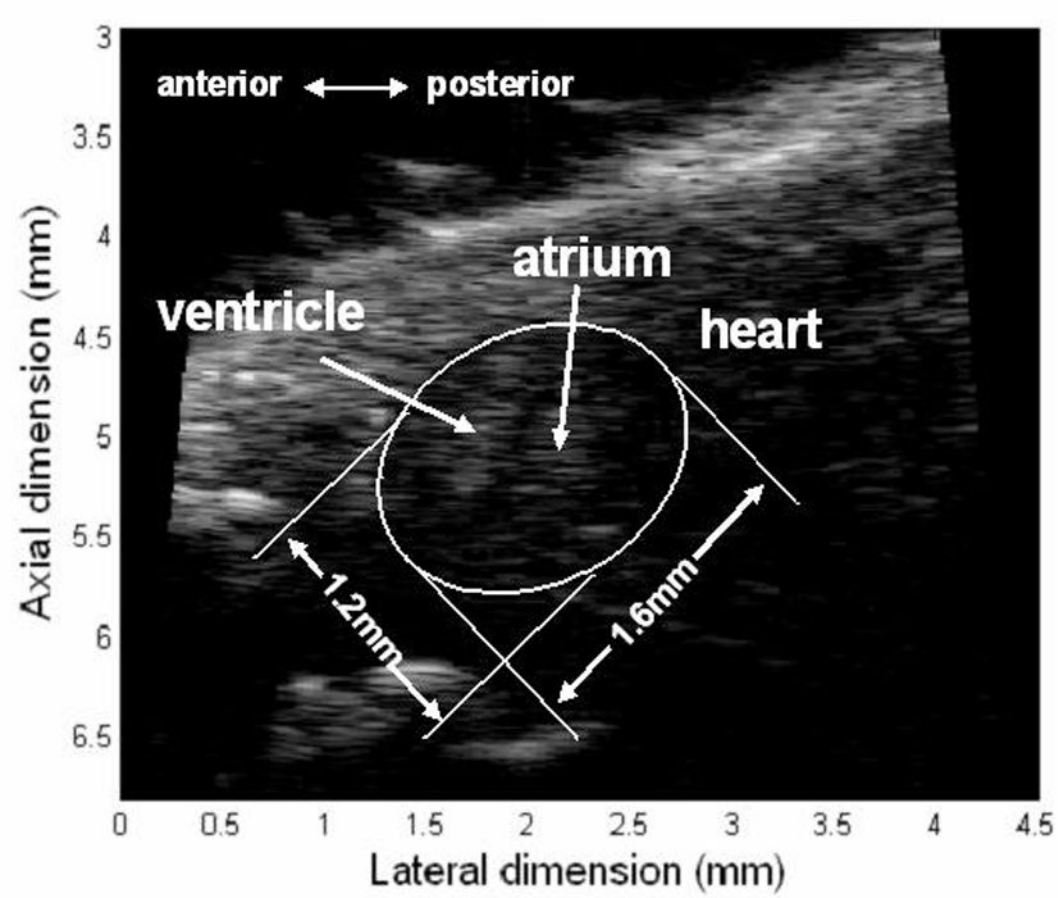

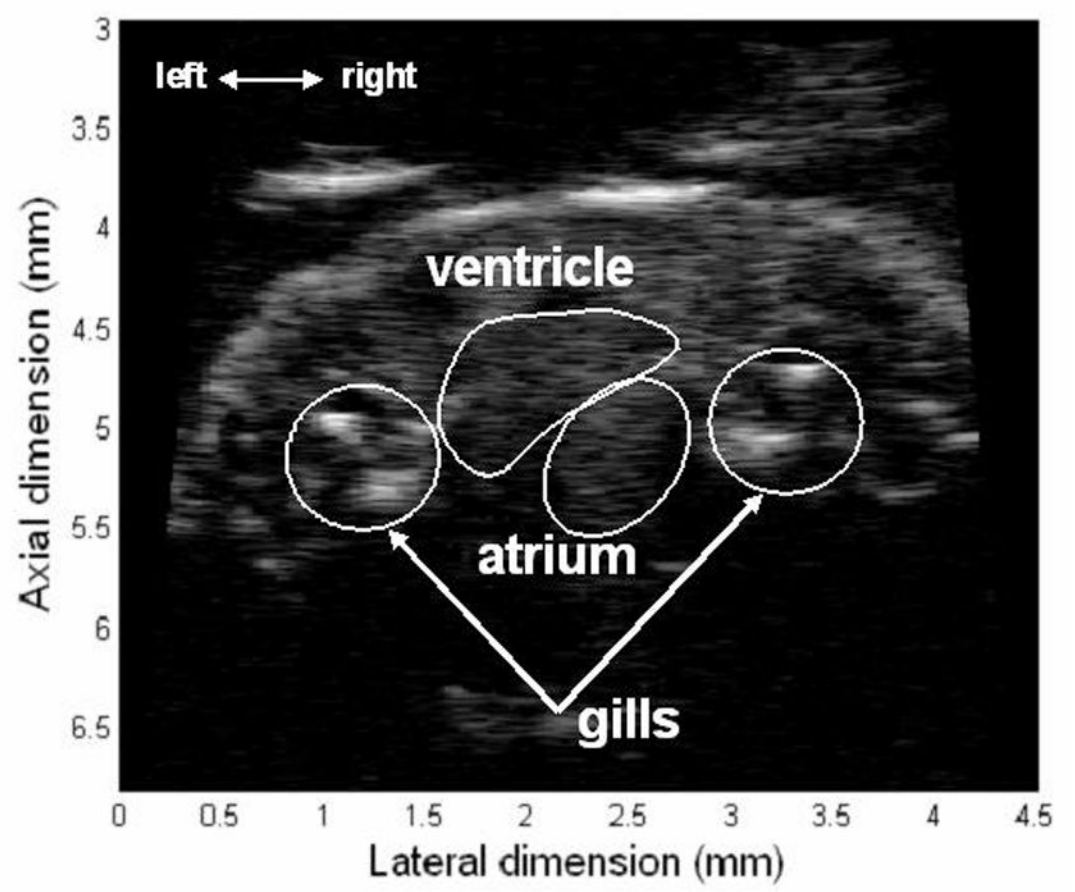

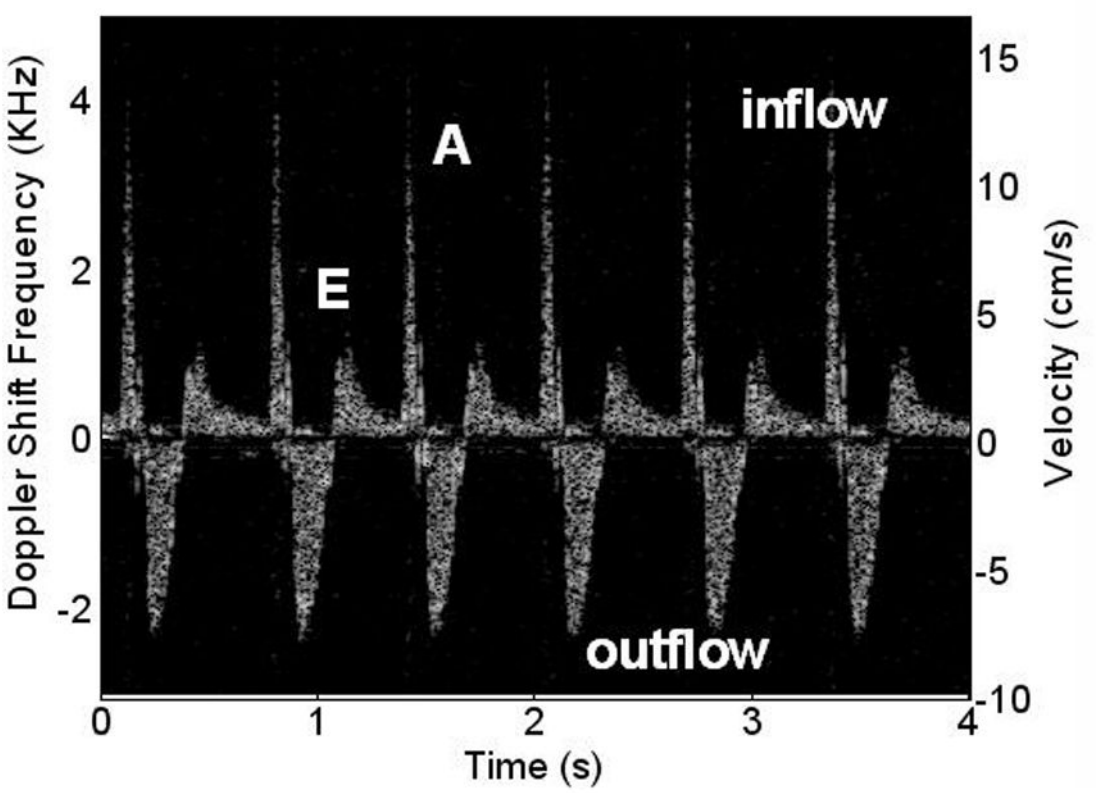

Figure 6.
UBM scans of an adult zebrafish heart at the isovolumic relaxation stage in an upside down position. (a) Sagittal view showing the atrium and ventricle located on the ventral side underneath the skin. The cardiac dimensions were 1.2 by 1.6 mm. (b) Transverse views displaying the heart positioned medially between the gills. (c) Pulsed-wave Doppler waveform of ventricular inflow (positive) and outflow (negative). The inflow consisted of early diastolic flow (E) and late diastolic flow (A).

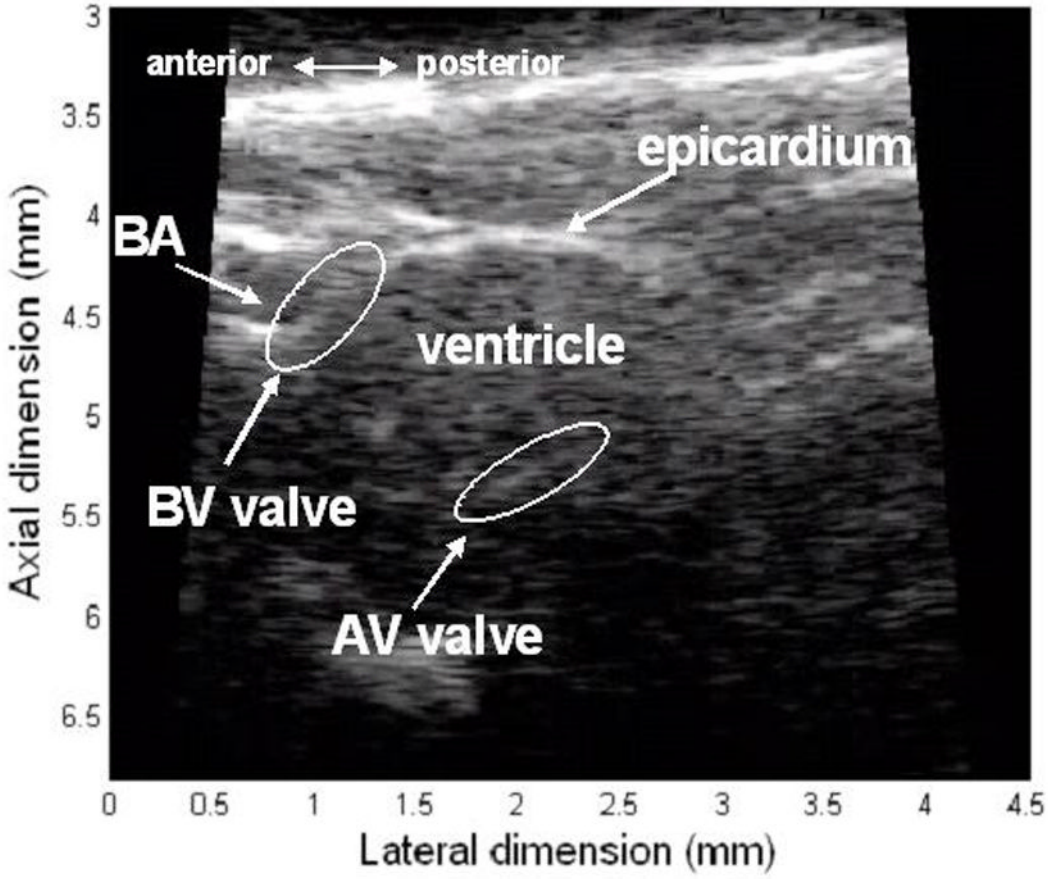

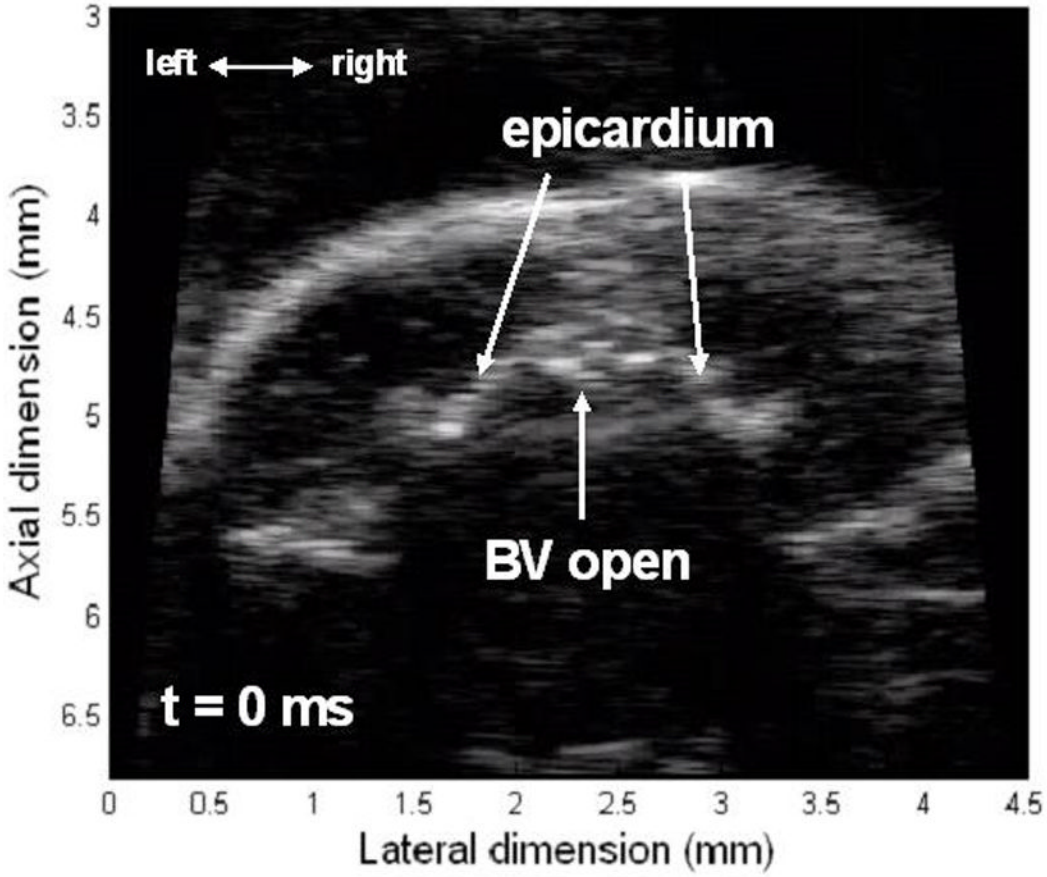

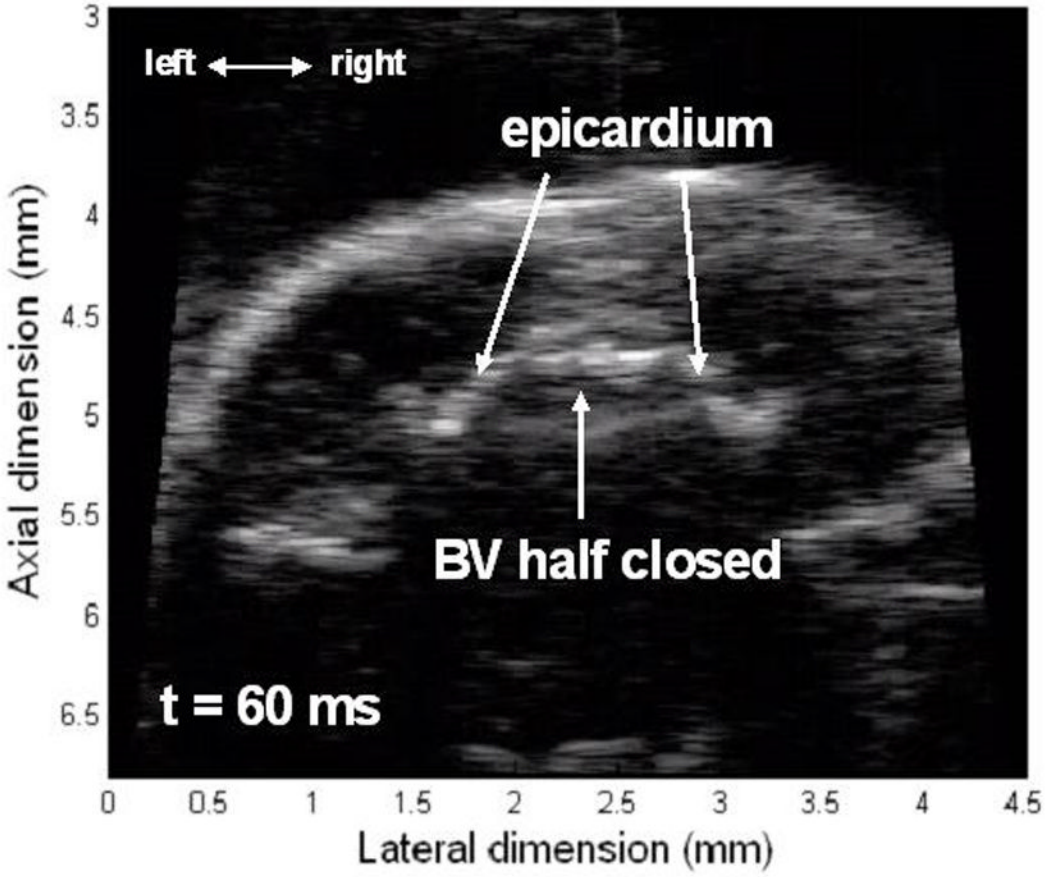

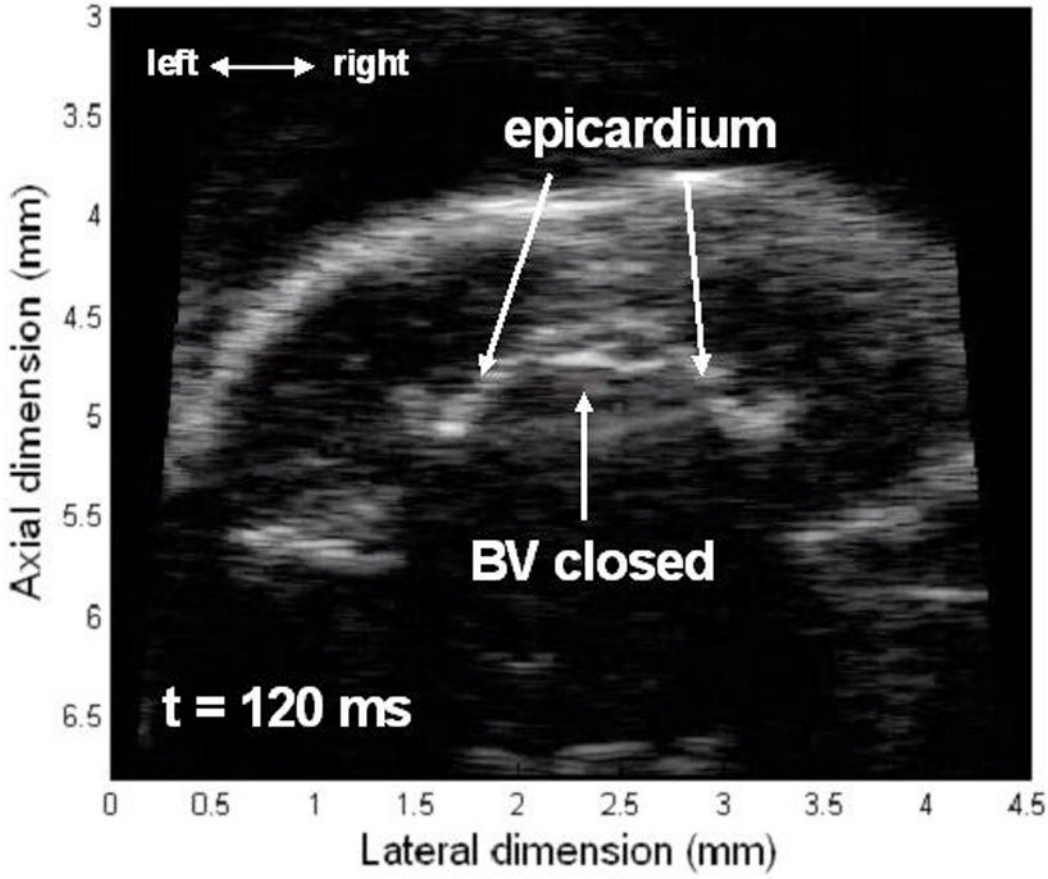

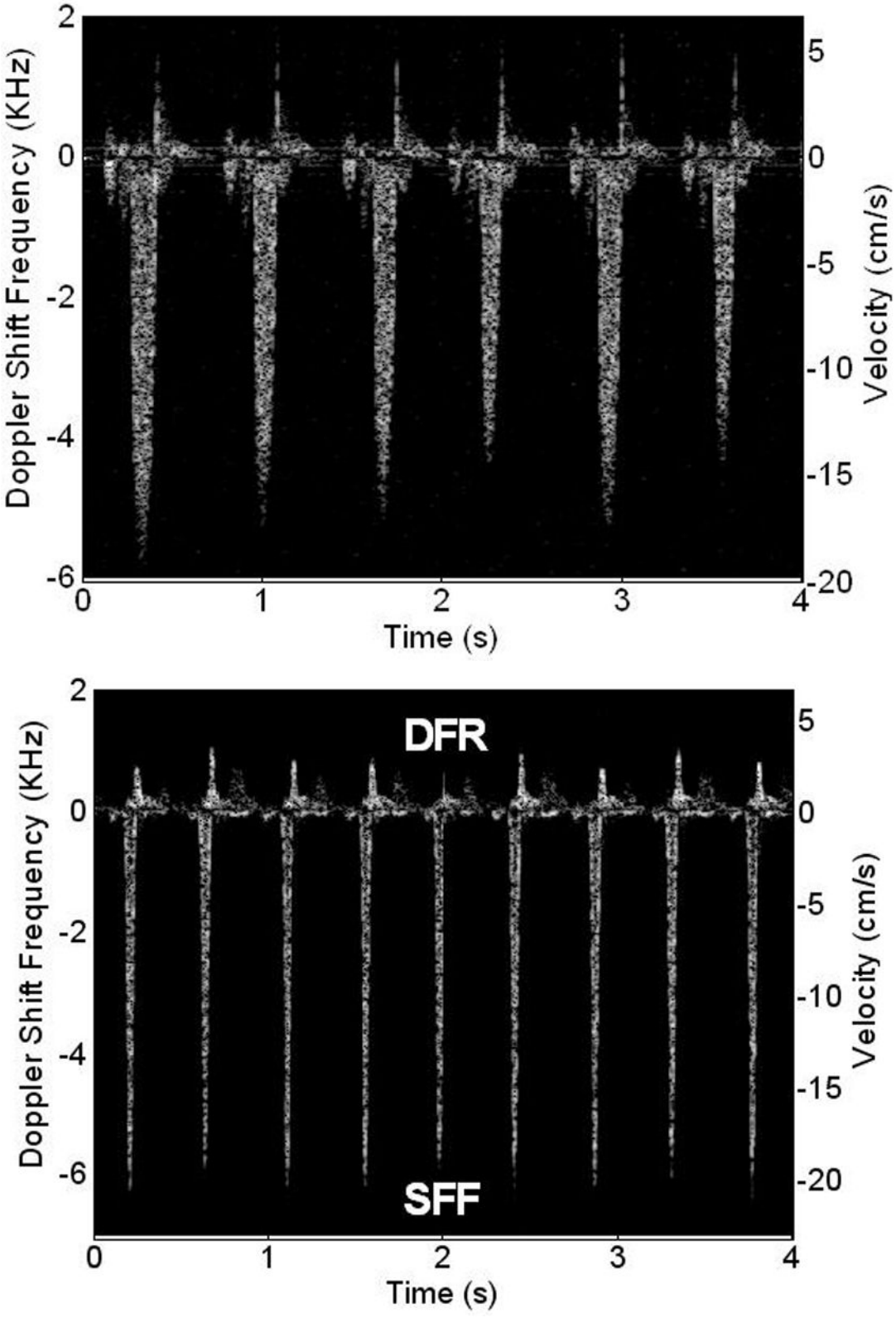

Figure 7.

(a) A sagittal view of the adult zebrafish heart at the isovolumic contraction stage showing the ventricle, bulbus arteriosus (BA), bulboventricular (BV) valve, atrioventricular (AV) valve, and epicardium. A series of transverse views of the BV valve at (b) open position, (c) half-closed position, and (d) closed position, at an interval of 60 ms. (e) Doppler waveform at medial BA. (f) Doppler waveform at posterior BA close to BV valve. In addition to systolic forward flow (SFF), diastolic flow reversal (DFR) appears when the ventricular pressure drops and blood flows backward.

Table 1

Zebrafish cardiac dimensions at isovolumic relaxation (IVR) and isovolumic contraction (IVC) stages (n=10).

Dimensions (mm × mm)	Value (mean ± SD)
Ventricle at IVR	1.24 ± 0.43 × 0.65 ± 0.30
Atrium at IVR	0.78 ± 0.21 × 0.54 ± 0.20
Ventricle at IVC	1.66 ± 0.48 × 0.79 ± 0.24
Atrium at IVC	0.64 ± 0.23 × 0.51 ± 0.19
Bulbus Arteriosus	0.48 ± 0.22 × 0.31 ± 0.15

Table 2

Doppler measurement of peak velocities and time durations in adult zebrafish heart (n = 10).

Parameters	Value (mean ± SD)
E-flow (cm/s)	3.6 ± 0.4
E-flow duration (ms)	320 ± 15
A-flow (cm/s)	14.4 ± 3.6
A-flow duration (ms)	110 ± 12
Outflow (cm/s)	8.0 ± 2.6
Outflow duration (ms)	200 ± 14
BA flow (medial) (cm/s)	16.0 ± 5.2
BA flow (posterior) (cm/s)	18.0 ± 4.9
Heart rate (beats per minute)	93 ± 25